Anomalous orbital dynamics in $LaSrMnO_4$ observed by Raman spectroscopy

K.-Y. Choi,[1] P. Lemmens,[2] D. Heydhausen,[3] G. Güntherodt,[3] C. Baumann,[4] R. Klingeler,[4] P. Reutler,[4] and B. Büchner[4]
[1]*National High Magnetic Field Laboratory, Tallahassee, Florida 32306-4390, USA*
[2]*Institute for Physics of Condensed Matter, TU Braunschweig, D-38106 Braunschweig, Germany*
[3]*II Physikalisches Institut, RWTH Aachen, 52056 Aachen, Germany*
[4]*Leibniz-Institute for Solid State and Materials, IFW Dresden, D-01171 Dresden, Germany*
(Received 2 September 2007; revised manuscript received 2 December 2007; published 12 February 2008)

We report inelastic light scattering experiments on the single-layered manganite $LaSrMnO_4$. The distinct features observed are the appearance of numerous symmetry-forbidden phonon peaks, with a strong temperature dependence of their intensity and frequency, and a double-peak structure of the activated high-frequency in-plane modes. These observations are ascribed to the conspicuous dynamics of an admixed $d_{x^2-y^2}$ orbital present in the background of the crystal field stabilized $d_{3z^2-r^2}$ orbitals. Our study suggests a significant competition between the kinetic energy gain due to the resulting orbital canting and the strong crystal field splitting.

DOI: 10.1103/PhysRevB.77.064415 PACS number(s): 75.47.Lx, 71.36.+c, 75.80.+q, 78.30.−j

I. INTRODUCTION

Orbital degrees of freedom are a key ingredient to understand competing interactions and novel phases in many transition metal oxides. A prototypical example is found in the three dimensional (3D) perovskite manganites where the interplay among spin, charge, and orbital degrees of freedom leads to a variety of competing phases.[1] In this respect, the single-layered manganite $LaSrMnO_4$ (LSMO) is a promising candidate because of its pronounced two-dimensional (2D) structural and electronic character. A lower dimensionality changes the orbital and spin dynamics. This can either related to more pronounced fluctuations or to lifting orbital degeneracies.[2,3] Also, the effect of doping in $La_{1-x}Sr_{1+x}MnO_4$ is different from the 3D counterpart as it does not show a ferromagnetic (FM) metallic phase. Instead, the observed spin glass and charge ordered phases indicate competing interactions.[4,5] Only for the case $x=0.5$, a well-defined charge and orbital ordering is realized that can be used as a reference material.[6] Interestingly, LSMO with different doping levels has recently been implemented in a device showing a colossal nonlinearity in electrical transport at the interface to a metal electrode.[7]

LSMO crystallizes in the same K_2NiF_4-type tetragonal structure ($I4/mmm$) with O(1) in-plane and O(2) apical oxygen sites as some high-T_C cuprates.[8] In LSMO, the MnO_2 magnetic layers are stacked along the c axis and separated by $(La,Sr)_2O_2$ planes leading to a ferro-orbital ordering of $d_{3z^2-r^2}$ orbitals and a C-type antiferromagnetic (AF) spin ordering below $T_N \approx 127$ K.[9–12] The question arises whether the orbital degrees of freedom are a relevant parameter to describe the properties of LSMO.

Anomalous, c-axis oriented remanent magnetic moments have been observed below 40 K together with a metastable behavior in μ-spin-relaxation measurements.[13,14] Also, the thermal length expansion has an additional anisotropic component. Finally, electron spectroscopy shows a temperature driven orbital occupation of diluted $d_{x^2-y^2}$ states in the background of the crystal field stabilized $d_{3z^2-r^2}$.[11,12,15,16] These so-called *canted states* couple strongly to the lattice. On the other hand, they are ferromagnetically correlated leading to the anomalous magnetization.[13] Recently, this view has been strongly supported by theory[4] emphasizing the competition between AF and FM degrees of freedom, which evolves with finite temperature.

In this paper, we present magnetic and phononic Raman scattering measurements of LSMO. We observe that with decreasing temperature, numerous symmetry-forbidden phonon peaks emerge while high-frequency in-plane modes split off. These features suggest the presence of a complex orbital dynamics in the background of the ferro-orbital ordered state of $d_{3z^2-r^2}$ type.

II. EXPERIMENTAL DETAILS

Single crystals of $LaSrMnO_4$ were grown using the floating zone method.[8] The samples from the same batch have been extensively characterized using neutron, magnetization, thermal expansion, x-ray absorption, and resistivity measurements.[8,11–13,15,16] Raman spectra were measured in a quasibackscattering geometry with the excitation line $\lambda = 532$ nm (2.33 eV) of a Nd doped yttrium aluminum garnet solid-state laser with the power of 8 mW and were collected by a Dilor-XY triple spectrometer and a nitrogen cooled charge-coupled device detector. The high-temperature measurements above 300 K were performed using a heating stage under vacuum.

III. RESULTS

Raman spectra in in-plane and interplane polarizations are shown in Fig. 1. For the space group $I4/mmm$, the factor group analysis yields four Raman-active phonon modes: Mn-O(2) and (La,Sr)-O(2) stretching modes have displacements along the c axis with A_{1g} symmetry and O(2) and (La,Sr) vibrations with displacements along the a and b axes with E_g symmetry.[17] The latter two, which are observable in (ca) light polarization, will not be discussed below since they do not add new physics. The pronounced peaks at 217 and 449 cm^{-1} observed in (cc) polarization correspond to the re-

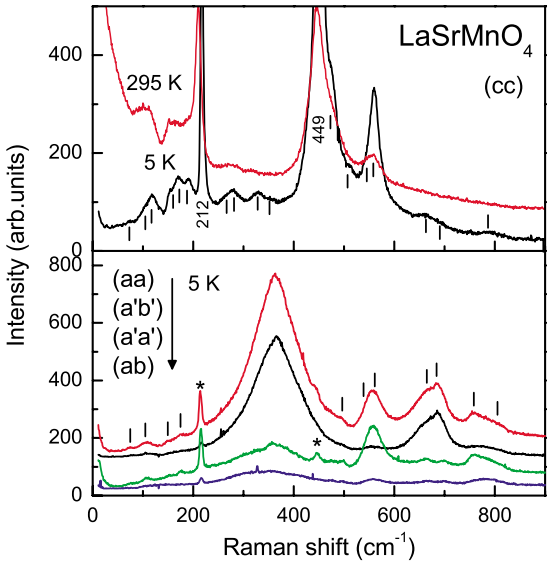

FIG. 1. (Color online) (a) Raman spectra in (cc) polarization at 5 and 295 K in LSMO. (b) Polarization dependence of Raman spectra at 5 K in (aa), $(a'b')$, $(a'a')$, and (ab) polarizations. Vertical bars denote symmetry-forbidden phonon peaks. Given numbers are phonon frequencies of the corresponding symmetry-allowed phonons. The broad maximum in (aa) and $(a'b')$ is assigned to two-magnon light scattering.

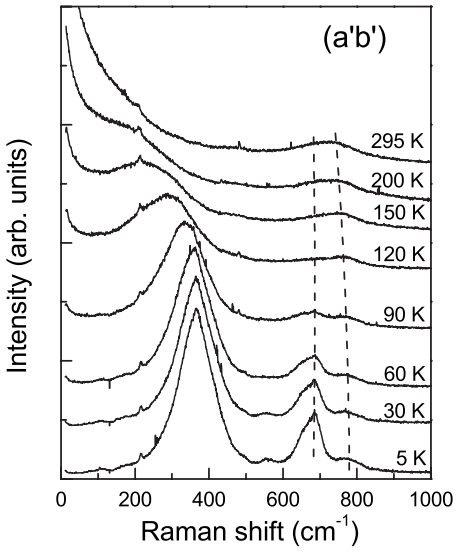

FIG. 2. Temperature dependence of two-magnon scattering in $(a'b')$ polarization in LSMO. The dashed lines are a guide for the eyes for the evolution of Mn-O(1) phonon modes.

spective (La,Sr)-O(2) and Mn-O(2) modes [see Fig. 1(a)]. In addition, at low temperatures, we observe numerous symmetry-forbidden phonon peaks at 73, 104, 118, 154, 171, 189, 219, 264, 278, 328, 356, 389, 449, 461, 507, and 768 cm^{-1}. Several of the additional peaks are still visible even at room temperature. These forbidden peaks are weak in intensity but show a well-defined symmetry as well as a significant temperature dependence in frequency and number (see Figs. 2 and 5). This rules out impurities and defects as a possible origin.

We now turn to the in-plane polarizations. Figure 1(b) displays the respective spectra in the four polarizations: (aa), (ab), $(a'b')=(a+b,a-b)$, and $(a'a')=(a+b,a+b)$, where a and b correspond to the polarization of incident and/or scattered light along the Mn-O(1) direction. These scattering geometries consist of spectra of the $A_{1g}+B_{1g}$, $A_{2g}+B_{2g}$, $B_{1g}+A_{2g}$, and $A_{1g}+B_{2g}$ symmetries, respectively. In the (aa) and $(a'a')$ polarizations, we observe weak A_{1g} phonon signals at the same frequencies of 217 and 449 cm^{-1} as in (cc) polarization (see the asteroids). This tells us that the Raman matrix element of $(A_{1g})_{ii}=(a,a,b)$ $(i=1-3)$ fulfills the condition of $a \ll b$.

In addition to the symmetry-allowed modes, a broad maximum around 356 cm^{-1} shows up in the (aa) and $(a'b')$ polarizations. It is strongly suppressed in the $(a'a')$ and (ab) polarizations. This selection rule suggests that the maximum has predominantly a B_{1g} symmetry character. We note that in strictly tetragonal symmetry, *magnetic* scattering is allowed in a B_{1g} symmetry. Thus, we assign the broad maximum to magnetic response. In (cc) polarization [Fig. 1(a)], quasielastic scattering appears at high temperatures but a magnetic continuum is absent at low temperature. This confirms the general validity of Raman scattering selection rules in LSMO.

Besides, the in-plane spectra exhibit numerous symmetry-forbidden phonon modes as the spectra of c-axis polarization show. The activated peaks are pronounced in the high-frequency range of 560–800 cm^{-1}. They are assigned to a bond bending and stretching mode of in-plane Mn-O(1) or MnO_6 octahedra. These frequencies are higher than 449 cm^{-1} of the Mn-O(2) mode because the Mn-O(1) distance is slightly shorter than the Mn-O(2) one. This assignment agrees well with previous experiments on $(La,Sr)MnO_3$ (Refs. 18 and 19) and $La_{0.5}Sr_{1.5}MnO_4$.[6] The activated low-frequency modes involve (La,Sr)-O(2) or only (La,Sr) and apical O(2) oxygen displacements since the bonding strength between the (La,Sr) and O(2) atoms is very weak. In this assignment, the strong high-frequency modes in in-plane polarization are associated with the high sensitivity of Mn-O(1)-type vibrations to electric fields along the in-plane direction. In contrast, for c-axis polarization, the low-frequency modes are largely stronger than the high-frequency ones except the 560 cm^{-1} mode possessing an A_{1g} symmetry. This confirms that the low-frequency modes pertain to apical O(2) oxygen displacements, which are intimately coupled to light with c-axis polarization. The exceptional behavior of the activated 560 cm^{-1} mode can be accounted for by considering the matrix element of the A_{1g} mode, which has a large c-axis component (see above).

First, we will discuss the detailed temperature dependence of the magnetic excitations (see Fig. 2). The maximum centered around 356 cm^{-1} shows a rather symmetric line shape at low temperatures. With increasing temperature, the spectrum broadens and shifts to lower energies. In particular, it undergoes a strong change around T_N and turns over to a wing feature of quasielastic scattering at higher temperature $(T \gg T_N)$. This is typical for two-magnon (2M) scattering originating from double spin-flip processes of an AF ground

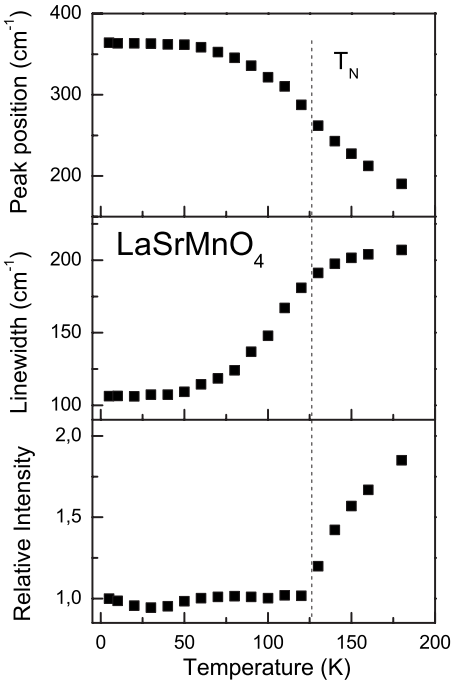

FIG. 3. Temperature dependence of the frequency, linewidth, and intensity of two-magnon scattering. The dotted vertical line marks T_N.

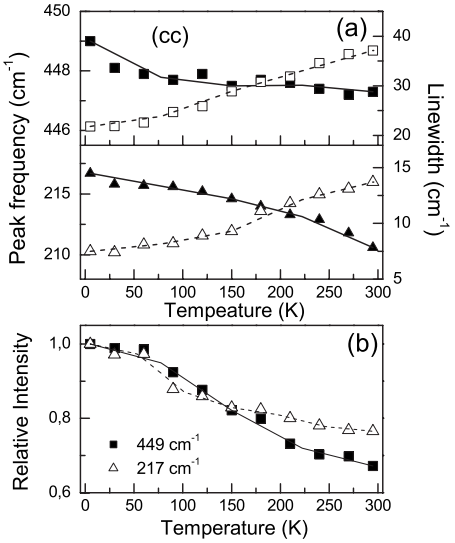

FIG. 4. (a) Temperature dependence of the frequency and linewidth of the 449 and 217 cm^{-1} modes in (cc) polarization. (b) Temperature dependence of the integrated intensity of the respective modes. Lines are guides for the eyes.

state $(S=2, S_z=\pm 2)$ to a higher state $(S=2, S_z=\pm 1)$.[20–22]

In the classical limit, the peak position of 2M scattering is given by $J_R(2zS-1)$, where J_R is the exchange constant between neighbor Mn spins, z is the number of nearest neighboring spins, and S is the spin quantum number.[21] For $S=2$ and $z=4$, we obtain $J_R=24$ cm^{-1} ($\approx$35 K). This value is in reasonable agreement with the inelastic neutron scattering result of $J_N \approx 39.8$ K.[10] The small discrepancy between these values might be due to deviations from the strict two dimensionality of the magnetic interactions.

Figure 3 summarizes the temperature dependence of the 2M frequency, linewidth at half maximum, and intensity of the 2M peak. The former two quantities are related with the evolution of short-wavelength magnon energies and lifetimes, respectively. The 2M frequency and linewith are determined directly from the peak position and the linewidth at half maximum. The intensity is obtained by integrating the spectrum in the frequency range of 15–500 cm^{-1}. At T_N, the peak frequency is renormalized by 20%. This value lies between that of 3D $S=1/2$ and 2D $S=1$ system.[21] Above T_N, the peak frequency drops off. The linewidth at half maximum exhibits a critical-type increase on approaching T_N. The scattering intensity is nearly constant in the ordered phase while increasing steeply above T_N.

Second, we address the symmetry-allowed modes at 217 and 449 cm^{-1} in (cc) polarization. Figure 4 displays the temperature dependences of the peak frequency, linewidth, and intensity. They show no appreciable anomalies around T_N. The peak energy of the 449 cm^{-1} mode exhibits little temperature dependence. With decreasing temperature, the 217 cm^{-1} mode hardens by 6 cm^{-1}, which is largely due to thermal contraction. For both modes, with decreasing temperature, the linewidth decreases quasilinearly and then tends to saturate at low temperature. This is typical for anharmonic lattice vibrations.[23] With increasing temperature, the scattering intensity decreases monotonically. Since insulating LSMO shows no drastic temperature dependence of a crystal structure and lattice parameters, the change of optical parameters is unlikely as possible sources. Here, we recall that the phonon intensity is influenced by (i) dependence of the band energy on the ion configuration and (ii) polarization of the band wave functions and the change in interionic distances. In LSMO, the out-of-plane $d_{3z^2-r^2}$ orbital character is enhanced at low temperatures due to an increase of the tetragonal distortion of the MnO_6 octahedron.[16] We thus assign the origin of the anomalies to a small change of the bond character.

Finally, we focus on the temperature dependence of the three activated modes at 551, 661, and 768 cm^{-1}. They commonly exhibit a double-peak structure with an energy splitting of 15–30 cm^{-1}. The former two modes are similar to excitations of $La_{0.5}Sr_{1.5}MnO_4$ with splittings that set in with the charge-exchange-type charge and orbital order.[6] However, this is totally unexpected in the undoped LSMO, which has no charge and orbital ordering superstructure.

We plot the integrated intensity and peak frequency of the respective modes as a function of temperature in Fig. 5. Both 551 and 661 cm^{-1} modes display a similar temperature dependence. Upon cooling through T_N, the peak frequency hardens by $\sim$20 cm^{-1} and then starts to saturate below 50 K. The integrated intensity of both modes undergoes a strong, monotonic increase upon cooling without obvious saturation even at the lowest temperature. This suggests that the appearance of the symmetry-forbidden modes is closely related to a magnetic ordering. In contrast to the 551 and 661 cm^{-1} modes, the 768 cm^{-1} mode persists to higher temperatures than T_N with a small level off of the intensity. With decreasing temperature, the frequency shows a small kink around T_N

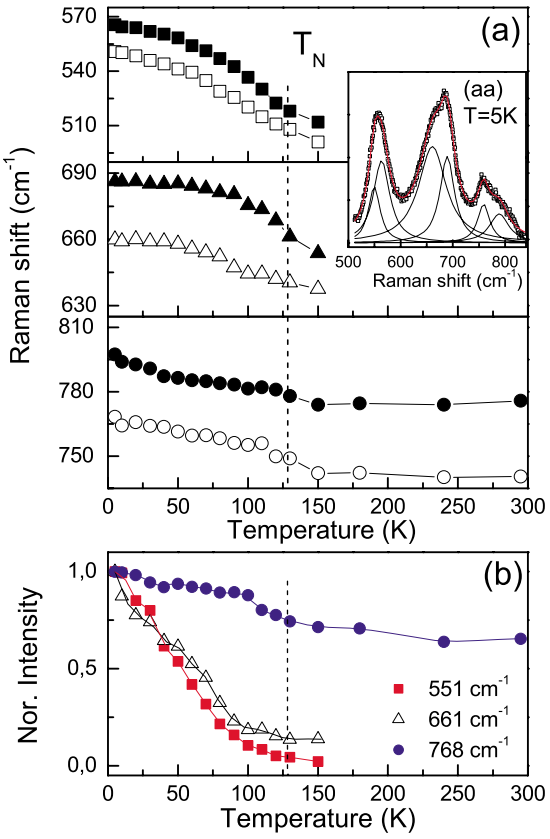

FIG. 5. (Color online) (a) Temperature dependence of the frequency of the Mn-O(1) vibrational modes at 551, 661, and 768 cm^{-1} in (*aa*) polarization. Inset: a fit of the Raman spectrum to a sum of the Lorentzian line profiles. (b) Temperature dependence of the integrated intensity of the respective vibrational modes. The intensity is normalized by the value of 5 K. Lines are guides for the eyes.

and shifts to higher energy quasilinearly. This mode seems to be less strongly coupled to spins.

IV. DISCUSSIONS

In the following, we will discuss the possible origin of the lattice anomalies. The appearance of the numerous symmetry-forbidden modes cannot be understood within structural changes, e.g., related to a tilting of the octahedra. Actually, the absence of a symmetry reduction has been pointed out in a detailed neutron diffraction study.[12]

For the case of the 3D manganite $(La,Sr)MnO_3$ and the half-doped 2D manganite $La_{0.5}Sr_{1.5}MnO_4$, it has been shown that orbitals strongly couple to the lattice.[18,19] This motivates us to attribute the symmetry-forbidden peaks to local lattice distortions induced by an orbital dynamics. In this case, the temperature dependence of their frequency and intensity can be used as a local, dynamical probe of the orbital state.

We recall that 15% of holes (85% of electrons) possess out-of-plane $d_{3z^2-r^2}$ orbital states, while the corresponding number of electrons occupy in-plane $d_{x^2-y^2}$ orbitals at room temperature.[15] This suggests that the orbital configuration is not determined exclusively by the tetragonal distortion of the octahedra. Thus, we are likely to invoke the transfer of $d_{x^2-y^2}$ orbitals to $d_{3z^2-r^2}$ to explain the observed lattice anomalies. However, a varying mixing degree of the two orbitals is not sufficient to account for the drastic change in number, frequency, and intensity of phonon modes with decreasing temperature through T_N (see Fig. 5). Rather, our study reveals a far more intriguing orbital dynamics than a simple orbital transfer.

The intimate correlation between the magnetic ordering and lattice anomalies highlights the important role of spin-orbital coupling in determining an orbital configuration. Such pure orbital couplings, on the one hand, push the electrons into the $d_{x^2-y^2}$ orbitals, which compensate crystal field effects. On the other hand, they can rearrange a $d_{x^2-y^2}$ orbital in a way to maximize the kinetic energy in the AF ordered state. Possibly, this leads to the nonuniform canted orbital states and their arrangements that deviate from a simple ferrodistortive form. Thus, we conclude that the lattice anomalies are associated with the intriguing behavior of the $d_{x^2-y^2}$ orbital, which is admixed to the dominant $d_{3z^2-r^2}$ orbital.

Furthermore, the splitting off of the activated high-frequency modes shows the presence of two different orbital states and accordingly two different charge carriers. This might be related to the two different (La,Sr) cations. In such a situation, the degree of covalency to O(1) in-plane oxygens depends on the orbital occupation of electron- and holelike carriers and leads to a gain of kinetic energy. Since they occupy different orbital states, the respective phonon modes involving Mn-O(1) vibrations will be split, as shown in the inset of Fig. 5. We thus relate this double-peak structure of each mode to two different charge carriers in different orbital states. The emergence of the numerous symmetry-forbidden peaks rules out the formation of a superstructure arising from a specific orbital ordering. Rather, the $d_{x^2-y^2}$ orbitals are in a disordered state at high temperatures, judging from the very weak intensity of the activated phonon peaks. The monotonic increase of the high-frequency mode intensity at low temperatures implies that the orbitals become more stabilized in favor of spin-orbital coupling but are not fully ordered.

We note that this scenario also explains the presence of ferromagnetic clusters. In the high-temperature paramagnetic phase, ferromagnetic correlations have been independently conjectured from magnetization measurements[11,13] and theoretical modeling.[4] The charge carriers with $d_{x^2-y^2}$ orbitals are coupled ferromagnetically to their neighboring Mn^{3+} ions since their orbitals are arranged in an orthogonal way. The charge carriers will form ferromagnetic clusters in order to gain double exchange energy. Our result suggests that the antiferrodistortive ordering of $d_{x^2-y^2}$ orbitals competes with the ferrodistortive ordering of $d_{3z^2-r^2}$ orbitals even in the AF ordered state. All these aspects demonstrate that pure orbital couplings should be considered beyond the crystal field effects to explain the anomalous magnetic and lattice behavior of LSMO.

V. CONCLUSIONS

In conclusion, we have reported Raman scattering measurements on the 2D single-layered manganite LSMO. All

features are described within a model based on an additional orbital disordered state present in the ferro-orbital ordered background. Our study emphasizes the significance of orbital coupling mechanisms in spite of the strong crystal field splitting, which give rise to a substantial orbital dynamics.

ACKNOWLEDGMENTS

We sincerely acknowledge fruitful discussions with M. Merz and financial support by DFG and the ESF program *Highly Frustrated Magnetism*.

[1] Y. Tokura and N. Nagaosa, Science **288**, 462 (2000).
[2] P. Lemmens, G. Güntherodt, and C. Gros, Phys. Rep. **375**, 1 (2003).
[3] P. Lemmens and P. Millet, in *Spin-Orbit-Topology, A Triptych In Quantum Magnetism*, edited by U. Schollwöck, J. Richter, B. J. J. Farell, and R. F. Bishop, Lecture Notes in Physics (Springer, Heidelberg, 2004).
[4] M. Daghofer, A. Oleś, D. Neuber, and W. vonder Linden, Phys. Rev. B **73**, 104451 (2006).
[5] M. Daghofer, D. R. Neuber, A. M. Oleś, and W. v. d. Linden, Phys. Status Solidi B **243**, 277 (2006).
[6] K. Yamamoto, T. Kimura, T. Ishikawa, T. Katsufuji, and Y. Tokura, Phys. Rev. B **61**, 14706 (2000).
[7] Y. Tokunaga, Y. Kaneko, J. P. He, T. Arima, A. Sawa, T. Fujit, M. Kawasaki, and Y. Tokura, Appl. Phys. Lett. **88**, 223507 (2006).
[8] P. Reutler, O. Friedt, B. Büchner, M. Braden, and A. Revcolevschi, J. Cryst. Growth **249**, 222 (2003).
[9] C. Baumann, G. Allodi, Büchner, R. De Renzi, P. Reutler, and A. Revcolevschi, Physica B **326**, 505 (2003).
[10] S. Larochelle, A. Mehta, L. Lu, P. K. Mang, O. P. Vajk, N. Kaneko, J. W. Lynn, L. Zhou, and M. Greven, Phys. Rev. B **71**, 024435 (2005).
[11] R. Klingeler, D. Bruns, C. Baumann, P. Reutler, A. Revcolevschi, and B. Büchner, J. Magn. Magn. Mater. **290-291**, 944 (2005).
[12] D. Senff, P. Reutler, M. Braden, O. Friedt, D. Bruns, A. Cousson, F. Bourée, M. Merz, B. Büchner, and A. Revcolevschi, Phys. Rev. B **71**, 024425 (2005).
[13] C. Baumann, G. Allodi, A. Amato, B. Büchner, D. Cattani, R. De Renzi, R. Klingeler, P. Reutler, and A. Revcolevschi, Physica B **374-375**, 83 (2006).
[14] D. Senff, Diploma thesis, University of Cologne, 2005; M. Braden and D. Senff, ILL Experimental Reports No. Ex 4-03-1358, 2003 (unpublished).
[15] M. Merz, P. Reutler, B. Büchner, D. Arena, J. Dvorak, Y. U. Idzerda, S. Tokumitsu, and S. Schuppler, Eur. Phys. J. B **51**, 315 (2006).
[16] M. Merz, G. Roth, P. Reutler, B. Büchner, D. Arena, J. Dvorak, Y. U. Idzerda, S. Tokumitsu, and S. Schuppler, Phys. Rev. B **74**, 184414 (2006).
[17] G. Burns, F. H. Dacol, and M. W. Shafer, Solid State Commun. **62**, 687 (1987).
[18] K. Y. Choi, P. Lemmens, G. Güntherodt, Yu. G. Pashkevich, V. P. Gnezdilov, P. Reutler, L. Pinsard-Gaudart, B. Büchner, and A. Revcolevschi, Phys. Rev. B **72**, 024301 (2005).
[19] K.-Y. Choi, Yu. G. Pashkevich, V. P. Gnezdilov, G. Güntherodt, A. V. Yeremenko, D. A. Nabok, V. I. Kamenev, S. N. Barilo, S. V. Shiryaev, A. G. Soldatov, and P. Lemmens, Phys. Rev. B **74**, 064406 (2006).
[20] P. A. Fleury and R. Loudon, Phys. Rev. **166**, 514 (1968).
[21] K.-Y. Choi, S. A. Zvyagin, G. Cao, and P. Lemmens, Phys. Rev. B **69**, 104421 (2004).
[22] M. G. Cottam and D. J. Lockwood, *Light Scattering in Magnetic Solids* (Wiley, New York, 1986).
[23] K.-Y. Choi, Yu. G. Pashkevich, K. V. Lamonova, H. Kageyama, Y. Ueda, and P. Lemmens, Phys. Rev. B **68**, 104418 (2003).